Available online at www.sciencedirect.com
SCIENCE DIRECT®
Journal of Molecular Catalysis A: Chemical 232 (2005) 59–67
JOURNAL OF MOLECULAR CATALYSIS A: CHEMICAL
www.elsevier.com/locate/molcata

An ONIOM study of amines adsorption in H-[Ga]MOR

Nan Jiang [a], Shuping Yuan [a], Jianguo Wang [a, *], Zhangfeng Qin [a], Haijun Jiao [a, b], Yong-Wang Li [a]

[a] *State Key Laboratory of Coal Conversion, Institute of Coal Chemistry, Chinese Academy of Sciences, P.O. Box 165, Taiyuan 030001, PR China*
[b] *Leibniz-Institute für Organische Katalyse an der Universität Rostock, Buchbinderstrasse 5-6, 18055 Rostock, Germany*

Received 27 September 2004; received in revised form 5 January 2005; accepted 6 January 2005

Abstract

The two-layered ONIOM method (B3LYP/6-31G(d,p):HF/3-21G) is used to study the interaction of amines (NH_3, $MeNH_2$, Me_2NH and Me_3N) with H-[Ga]MOR. The optimization of the local structure of H-[Ga]MOR cluster leads to two stable bridging hydroxyl sites ($O_{10}H$ and O_2H) in the zeolite framework, being different from that of H-[Al]MOR. In the adsorption complexes, all amines are protonated by the acidic proton of H-[Ga]MOR, and the protonated amines (HNR_3^+) are stabilized by hydrogen bonds between the negatively charged zeolite oxygen atoms and the hydrogen atoms of the N–H and C–H bonds in the adsorbates. This interaction is confirmed by the structure of the adsorption complexes as well as the calculated IR stretching frequencies. The calculated adsorption energies of amines agree reasonably with the available experimental data. It is found that NH_3 prefers to adsorb at the O_2H Brønsted site, while Me_2NH and Me_3N prefer to adsorb at the $O_{10}H$ site, and $MeNH_2$ can be in equilibrium between O_2H and $O_{10}H$. The relative order of the basicity of amines on the basis of the computed adsorption energies agrees well with the experiments, but differs from those in the gas phase (proton affinity) and in solvents (pK_a).

Keywords: Amines; Adsorption; H-[Ga]MOR; ONIOM; IR frequency

1. Introduction

Zeolites are extensively used as catalysts for chemical industries due to their Brønsted acidity and shape-selectivity. For zeolites to have desired catalytic activity, selectivity and stability, it is necessary to modify the pore structure and the acidity by incorporation of other elements, such as B, Ga, Fe, etc. into the framework. For example, Ga modified HZSM-5 is very efficient for alkylation of benzene with propene [1], TS-1 zeolites are known for their increased catalytic activity in selective oxidation [2], and MFI type zeolite containing Fe element in its framework shows good performance in benzene oxidation [3].

The acidity of zeolites is experimentally estimated by studying the adsorption of probe molecules such as ammonia [4,5] and pyridine [6,7] on their bridging hydroxyl groups using IR and NMR spectroscopic methods. This interaction within zeolite is a critical step in the catalytic process, and strongly affects the catalytic activity and selectivity of reaction and separation efficiency. Thus a better understanding of adsorption behavior of probe molecules in zeolites is of considerable importance for adsorptive and catalytic properties of zeolites. As a result, the investigations of base molecules adsorbed in the acid center have been the topic of many studies, i.e. chemisorption of base molecules studied by temperature-programmed desorption to obtain information of the acid sites.

NH_3 is one of the most frequently used probe molecule for the acidity of zeolite. It becomes NH_4^+ in H-type zeolites and there formed several N–H···O hydrogen bonds in the [$ZeO^-\cdots NH_4^+$] ion-pair. The successive replacement of hydrogen atoms in NH_3 by methyl groups can produce three amines ($MeNH_2$, Me_2NH and Me_3N) with enhanced basicity and bulky structures, which are expected to have different types and strength of interactions with the zeolite framework.

* Corresponding author. Tel.: +86 3514046092; fax: +86 3514161578.
E-mail address: iccjgw@sxicc.ac.cn (J. Wang).

1381-1169/$ – see front matter © 2005 Elsevier B.V. All rights reserved.
doi:10.1016/j.molcata.2005.01.025

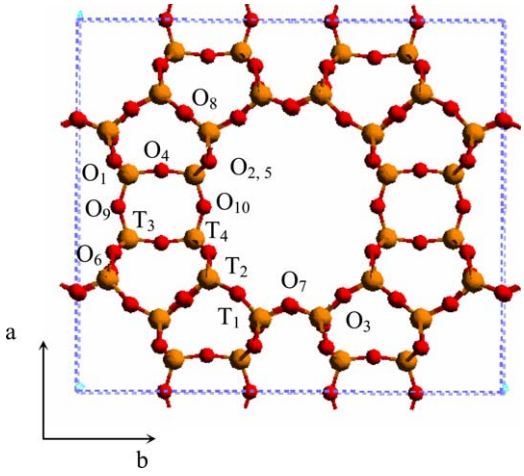

Fig. 1. The structure of mordenite unit-cell viewed down the *c*-axis (T_1–T_4 and O_1–O_{10} are designated. Note that O_2 and O_5 sites are superposed in a projection along the *c*-axis).

This is clearly shown by the study of Su and coworkers [8,9] on the interaction of $MeNH_2$ with several alkali cation exchanged large pore zeolites.

A number of theoretical methods have been proposed to study the interaction of base molecules with zeolite. In order to model the features of real systems, a large enough system and highly accurate ab initio method should be used. However, application of accurate ab initio methods to large system is time-exhausting and sometimes impossible. An effective method to this problem is the hybrid method, such as embedding method [10,11] or the combined quantum mechanical and molecule mechanical method (QM/MM) [12,13]. Sauer et al. have successfully used PM-Pot scheme on ZSM-5 [14,15], as well as the more general ONIOM method by Morokuma and coworkers [16–18] has brought accurate results to large systems. For example, Kasuriya et al. have successively applied ONIOM method to the interaction of aromatic hydrocarbons with H-FAU [19]. It is also applied to the study of chemical reactions [20–22].

In this work, we focus on mordenite (MOR), which is a particularly useful catalyst for several applications including cracking and isomerization of *n*-alkanes [23,24]. It has been shown that the elements such as B, Ga, and Zn, can be introduced into the MOR framework [25,26]. As shown in Fig. 1, MOR has a multiple pore-system with main channels of 12-membered rings that are connected by 8-membered rings. In the unit cell, there are 10 different oxygen sites (O_1–O_{10}) and four crystallographic different tetrahedral sites (T sites, T_1–T_4) at which Al or Ga can be substituted. Earlier theoretical study showed that Ga prefers T_4 site when replacing Si in the MOR framework [27]. Here we use the two-layered ONIOM (ONIOM2) method to study the structure of H-[Ga]MOR, and its interaction with different amines (NH_3, $MeNH_2$, Me_2NH and Me_3N). The adsorption energies and the IR frequencies are satisfactorily compared with the experimental data. The goal of this work is to correlate the type and strength of interaction of H-[Ga]MOR with different amines. This provides the opportunity to develop new probe molecules for acidity and basicity of zeolites.

2. Models and methods

2.1. Models

The coordination of the atoms in this work is taken from the structure of Na-MOR [28]. A 20T model is employed to represent the acid sites and pore structure of MOR, as shown in Fig. 2a, which contains 20 SiO_4 tetrahedron centers (20T) and includes a complete two-layered 12-membered ring. In this cluster a Ga atom replaces the Si atom at one of the T_4 site. To maintain the charge neutrality of the cluster, a charge-balancing proton is produced. The proton was initially put in a position where it is at almost the same distance from the three oxygen atoms around the Ga center. The optimization of this initial structure leads to two stable clusters A and B (see Fig. 2b and c), in which the charge-compensating proton is attached to O_{10} and O_2, respectively. Terminal hydrogen atoms are used to saturate the peripheral oxygen atoms in the cluster. The O–H distances are 1.0 Å, and the orientation of O–H bonds is along the pre-existing O–Si bonds. The clusters simulating the amine adsorption in H-[Ga]MOR are constructed by the partially optimized 20T clusters of H-[Ga]MOR and the free optimized amines. The amine molecules are put pointing to the 12-membered ring with the nitrogen atom closing to the acidic proton (Hz).

2.2. Methods

All calculations in this work are performed by using Gaussian 03 program [29] and the ONIOM2 method. In this ONIOM model, the whole system is divided into two different layers, which are described by two different methods. In the bare cluster of H-[Ga]MOR, the 6T model (shown as ball and stick in Figs. 2–4) forming the high-layer is described at B3LYP/6-31G(d,p) level, and the rest of the clusters forming the low-layer is treated at HF/3-21G level. In the adsorbed complexes, the probe molecules are also included in the high-layer, and this ONIOM2 model can ensure that all the interactions between the adsorbates and zeolite frameworks are included in the high-layer. In order to avoid chemical unreality, three linking H atoms are introduced to replace Si atoms between two layers.

The 20T cluster for the structures of H-[Ga]MOR is partially optimized with the acid sites and their neighboring Si and Ga as well as the oxygen atoms surrounding Ga relaxed, while the rest atoms are fixed to their crystal positions, respectively. To optimize the adsorbed complexes, the parameters of the adsorbate molecule and the atoms described above in the bare H-[Ga]MOR clusters are relaxed with the rest of the clusters fixed.

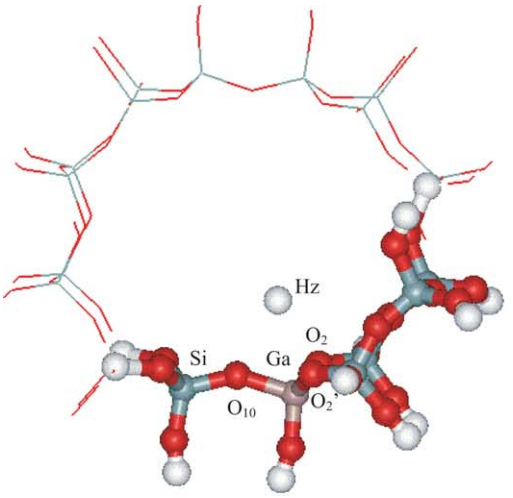

(a)

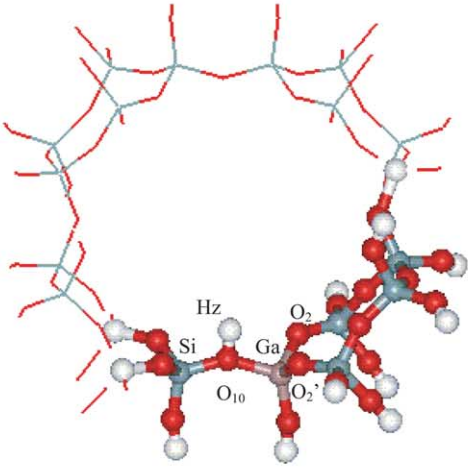

(b) (cluster **A**)

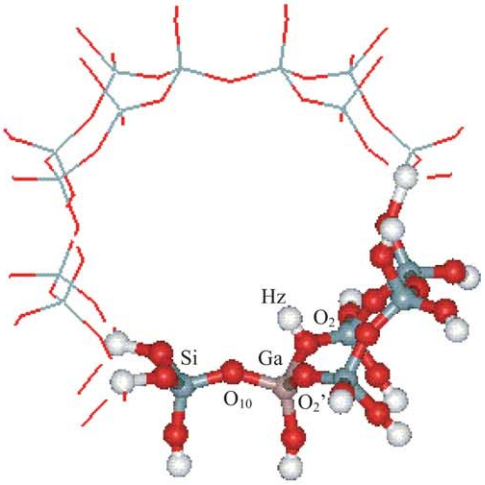

(c) (cluster **B**)

Fig. 2. 20T clusters simulating the structure of H-[Ga]MOR: (a) initial structure; (b) cluster A with charge-compensating proton attached to O_{10}; (c) cluster B with charge-compensating proton attached to O_2.

The adsorption energy (ΔE_{ads}) is defined as the energy difference between the adsorption complexes and the individual 20T cluster and amine molecule, and is calculated by: $\Delta E_{ads} = (E_{adsorbate} + E_{20T}) - E_{20T\text{-}adsorbate}$. To calculate IR frequencies of the adsorbed states, the 6T clusters cut from the high-layer of the ONIOM2 adsorption complexes (see Fig. 5) are used. Geometry optimizations and frequency calculations on these 6T complexes are performed at B3LYP/6-311G(d,p) level, and all calculated frequencies given in this work are scaled by 0.9613 [30].

3. Results and discussion

3.1. The local structure of H-[Ga]MOR

Table 1 presents the calculated bond lengths of the local structure of clusters A and B with Brønsted acid site located in O_{10} and O_2 sites. It is shown that the distance between Ga and the hydroxyl oxygen atom (R_{Ga-O10} and R_{Ga-O2}) is longer than the other two Ga–O bonds in both A and B, indicating that the attaching of the charge-compensating proton somewhat affects the fine structure of the zeolite around it. It is also found that the bond length of the bridging hydroxyl group (R_{O10-Hz}) in A is 0.004 Å longer than that (R_{O2-Hz}) in B, which means that the acidity of A is stronger than that of B. However, B is computed to be more stable than A by 3.6 kcal/mol (Table 1), indicating that B is more energetically favored than A. This should be the upper limit of the energy difference between two hydroxyl bridged structures. Under fully relaxation and without any constrains, this difference will become small, indicating the possible equilibrium of these two structures [31].

3.2. Adsorption of amines in A

The structure of the amines adsorption complexes based on cluster A is shown in Fig. 3 and the bond length parameters are reported in Table 2. As found in a previous work [32], NH_3 becomes NH_4^+, and there are three NH···O hydrogen bonds between hydrogen atoms of NH_4^+ and the zeolite framework. Upon the adsorption of amines, the distance between bridging oxygen atom and charge-compensating proton (R_{O10-Hz}) has changed from 0.980 to 1.717–2.031 Å,

Table 1
Selected bond lengths (Å) of the Brønsted sites in clusters A and B and their relative total energies[a]

	A ($O_{10}H$)	B (O_2H)
R_{O10-Hz} (R_{O2-Hz})	0.980	(0.976)
R_{Ga-O10} (R_{Ga-O2})	1.820	(1.928)
R_{Ga-O2} ($R_{Ga-O2'}$)	1.780	(1.820)
$R_{Ga-O2'}$ (R_{Ga-O10})	1.776	(1.743)
$E_{relat.}$ (kcal/mol)[b]	0.0	−3.6

[a] The numbering of the atoms follows the crystallographic number designated in Fig. 2.

[b] The relative total energy of clusters A and B.

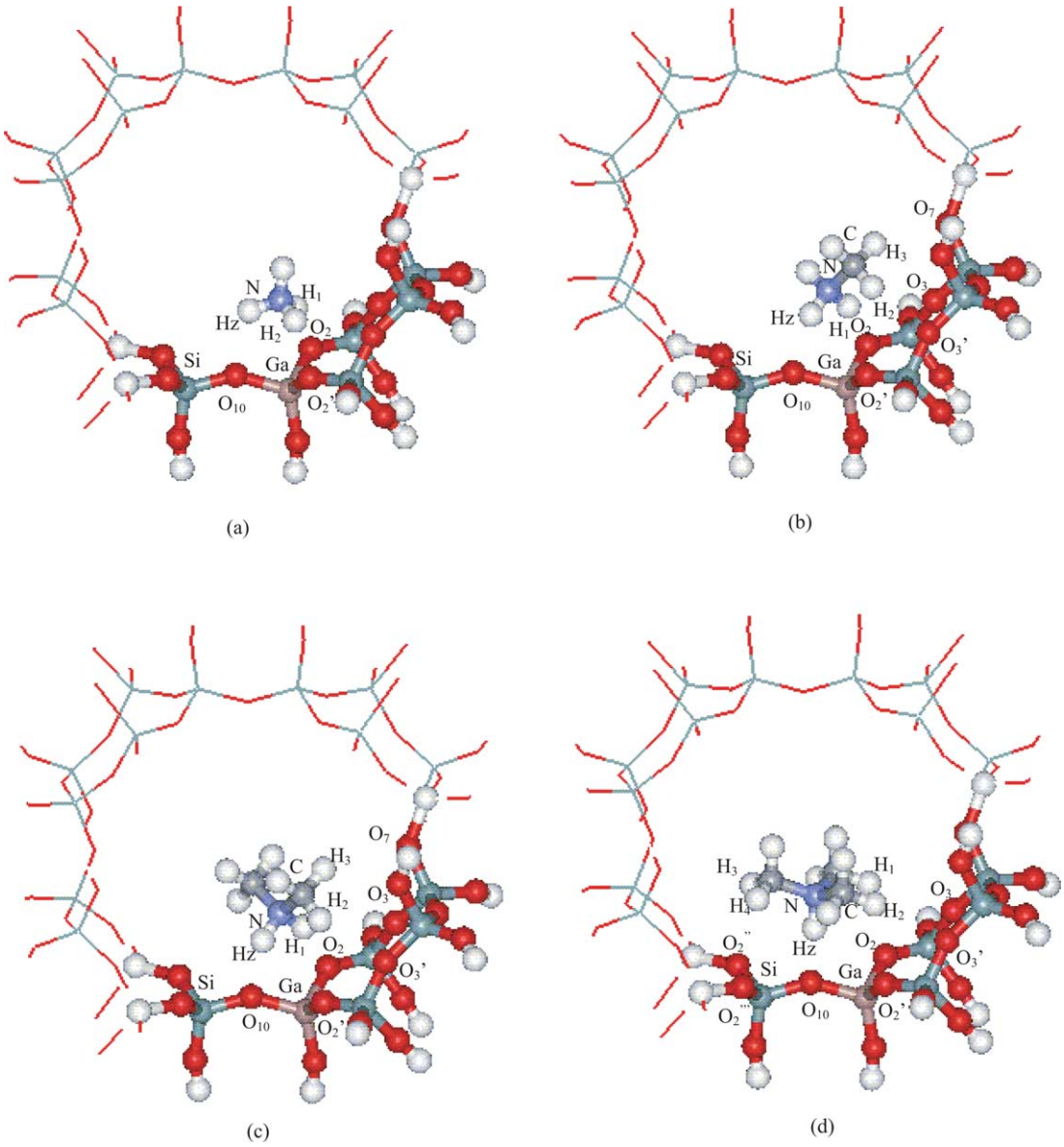

Fig. 3. Structures of the adsorption complexes of amines in A: (a) NH_3/A; (b) $MeNH_2$/A; (c) Me_2NH/A; (d) Me_3N/A.

and the distance between the amine nitrogen atom to proton becomes1.036–1.060 Å. These data indicate that the proton has been transferred from the Brønsted acidic sites of the zeolite framework to the adsorbed amines to form ammonium ions ($[HNR_3]^+$), and there is strong hydrogen bond interaction between the protonated amines and the negatively charged zeolites framework with O–H distances ranging from 1.717 to 2.031 Å.

In addition to this interaction, there exist additional hydrogen bonds between these ion-pair structures. In $MeNH_2$, Me_2NH and Me_3N molecules, since one or more hydrogen atoms are substituted by methyl groups, producing molecules with larger size as compared with NH_3, and therefore more hydrogen atoms become closer to oxygen atoms of the zeolite framework. Apart from the interactions between lattice oxygen atoms and the hydrogen atoms bonded to nitrogen, the hydrogen atoms of the methyl groups can also interact with zeolite lattice oxygen atoms, i.e. $[HNR_3]^+$ is stabilized by NH···O and CH···O hydrogen bonds through the negatively charged framework. The NH···O bond lengths of 1.642–1.692 Å are much shorter than that of the CH···O bonds of over 2.5 Å, indicating that the NH···O bonds are stronger than the CH···O bonds.

As a result of these interactions, the N–H and C–N bonds of $[HNR_3]^+$ are elongated and the C–H bonds become shorter as compared with those of the free NR_3 molecules. For $[MeNH_3]^+$ and $[Me_2NH_2]^+$ there are two strong CH···O hydrogen bonds, as found in the distances of $R_{O10—Hz}$ (2.031 and 1.864 Å) and $R_{O2—H1}$ (1.642 and 1.692 Å).

From the structure of the adsorption complexes (Fig. 3) and the structural parameters reported in Table 2 it can be found that the main interactions between the $[HNR_3]^+$ and

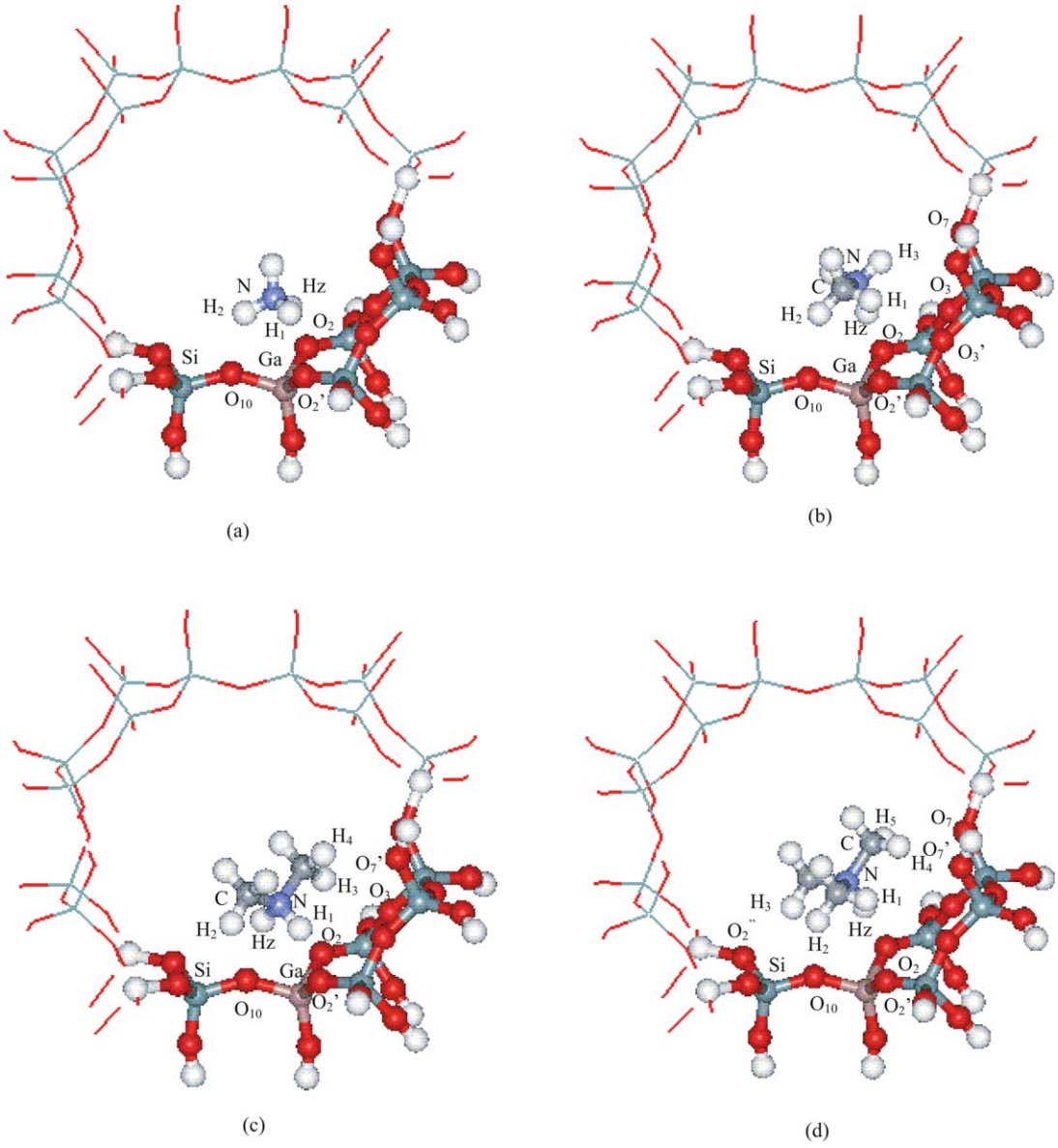

Fig. 4. Structures of the adsorption complexes of amines in B: (a) NH_3/B; (b) $MeNH_2$/B; (c) Me_2NH/B; (d) Me_3N/B.

the zeolite substrates are included in the high-layer of the ONIOM2 models, indicating that the ONIOM2 models used in the present work are efficient in studying the adsorption of amine molecules in H-[Ga]MOR zeolite.

3.3. Adsorption of amines in B

The structure of the amines adsorption complexes based on cluster B is shown in Fig. 4 and the bond length parameters are listed in Table 3. Similarly to the adsorption in cluster A, all the amine molecules are protonated in B, and there are hydrogen bonds interactions between the formed $[HNR_3^+]$ and the negatively charged zeolite framework. Among the formed hydrogen bonds, the NH···O interactions with O–H bond lengths of 1.526–2.051 Å are stronger than the CH···O interactions with O–H bond lengths of 2.453–2.936 Å.

It is interesting to compare the energy difference between different amines adsorbed on A and B (Table 4). It is found in a previous part that the bare B is more stable than A by 3.6 kcal/mol. As for the adsorption complexes, $[NH_4]^+$/B is also more stable than $[NH_4]^+$/A by 2.3 kcal/mol. However, both $[MeNH_3]^+$/B and $[MeNH_3]^+$/A have the same energy. With two and three methyl groups replaced hydrogen atoms, $[Me_2NH_2]^+$/B and $[Me_3NH]^+$/B are less stable than $[Me_2NH_2]^+$/A and $[Me_3NH]^+$/A by 7.3 and 4.1 kcal/mol, respectively. This energetic change shows the effect of the introduced methyl groups to amine molecules and the type and strength of the interaction between $[R_3NH]^+$ and the zeolite framework upon the changes of the structure of probe molecules. It is clearly shown that NH_3 prefers to be adsorbed on the acidic site in B, while Me_2NH and Me_3N prefer to be adsorbed on the acidic site in A, and $MeNH_2$ can be

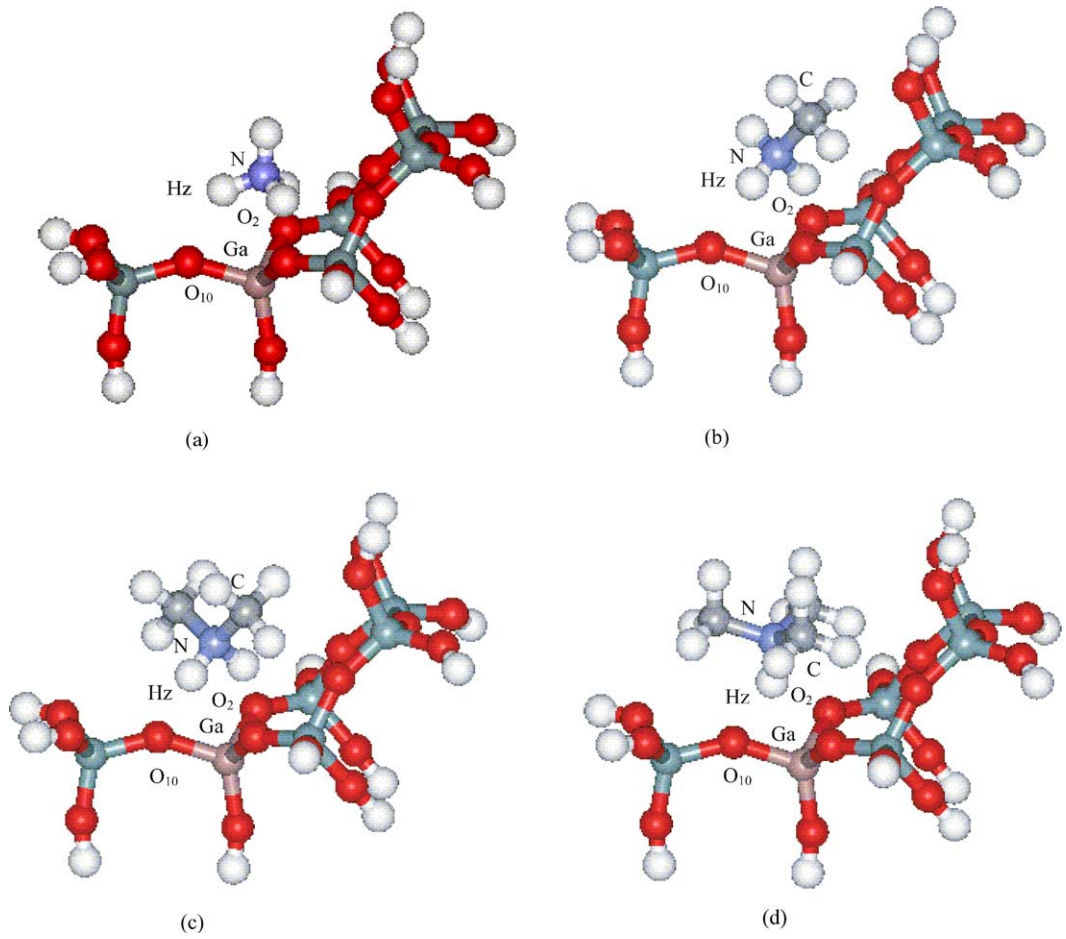

Fig. 5. The 6T cluster models used for frequency calculations of the adsorption complexes: (a) NH_3/6T; (b) $MeNH_2$/6T; (c) Me_2NH/6T; (d) Me_3N/6T.

Table 2
The selected bond lengths (Å) of the amines adsorption complexes in cluster A[a]

	NH_3/A	$MeNH_2$/A	Me_2NH/A	Me_3N/A
$R_{O10—Hz}$	2.126	2.031	1.864	1.717
$R_{Ga—O10}$	1.766	1.770	1.776	1.780
$R_{Ga—O2}$	1.869	1.871	1.870	1.843
$R_{Ga—O2'}$	1.863	1.841	1.838	1.836
$R_{N—Hz}$	1.030	1.036	1.042	1.060
$R_{O2—H1(N)}$ ($R_{O2—H1(C)}$)	1.730	1.642	1.692	(2.406)
$R_{O2'—H2(N)}$ ($R_{O2'—H2(C)}$)	1.875	(2.820)	(2.610)	(2.534)
$R_{O3'—H2(C)}$	–	2.426	2.584	2.762
$R_{O7—H3(C)}$ ($R_{O2''—H3(C)}$)	–	2.660	2.972	(2.728)
$R_{O3—H1(N)}$ ($R_{O3—H1(C)}$)	–	2.832	2.935	(2.822)
$R_{O2'—Hz}$ ($R_{O2'''—H4(C)}$)	–	–	2.922	(2.810)
$R_{N—H}$(av.)[b]	1.028 (1.018)	1.032	1.056	–
		(1.017)	(1.017)	
$R_{C—N}$(av.)[b]	–	1.493	1.488	1.496
		(1.465)	(1.457)	(1.455)
$R_{C—H}$(av.)[b]	–	1.090	1.091	1.090
		(1.098)	(1.099)	(1.099)

[a] The numbering of the atoms follows those designated in Fig. 3.
[b] The average length of all N—H, C—N or C—H bonds, respectively, in the adsorbed state, and the data in parentheses are the values of the free molecules.

Table 3
The selected bond lengths of the amines adsorption complexes in cluster B[a]

	NH_3/B	$MeNH_2$/B	Me_2NH/B	Me_3N/B
$R_{O2—Hz}$ ($R_{O10—Hz}$)	1.665	1.526	2.235 (1.995)	1.726
$R_{Ga—O2}$	1.885	1.898	1.862	1.891
$R_{Ga—O2'}$	1.847	1.838	1.855	1.838
$R_{Ga—O10}$	1.765	1.841	1.838	1.764
$R_{N—Hz}$	1.068	1.090	1.030	1.062
$R_{O2'—H1(N)}$ ($R_{O2'—H1(C)}$)	1.993	(2.636)	1.768	(2.755)
$R_{O10—H2(N)}$ ($R_{O10—H2(C)}$)	2.051	(2.453)	(2.770)	(2.268)
$R_{O2'—H2(C)}$	–	2.923	–	–
$R_{O3'—H1(C)}$	–	2.736	–	–
$R_{O3—H3(N)}$ ($R_{O3—H3(C)}$)	–	2.881	(2.508)	–
$R_{O7'—H4(C)}$ ($R_{O2'—H3(N)}$)	–	–	2.936	(2.297)
$R_{O7—H3(N)}$ ($R_{O7—H4(C)}$)	–	2.796	–	(2.382)
$R_{O10—Hz}$ ($R_{O7'—H4(C)}$)	–	–	1.950	(2.782)
$R_{N—H}$(av.)[b]	1.029	1.023	1.052	–
	(1.018)	(1.017)	(1.017)	
$R_{C—N}$(av.)[b]	–	1.499	1.488	1.496
		(1.465)	(1.457)	(1.455)
$R_{C—H}$(av.)[b]	–	1.089	1.090	1.090
		(1.098)	(1.099)	(1.099)

[a] The numbering of the atoms follows those designated in Fig. 4.
[b] The average length of all N—H, C—N or C—H bonds, respectively, in the adsorbed state, and the data in parentheses are the values of the free molecules.

in equilibrium between A and B. Based on these data, it can be declared that the ammonium ions ($[R_3NH]^+$) interact with the negatively charged (deprotonated) A more strongly than B. This is also reflected by the adsorption energies discussed in the next part.

3.4. Adsorption energies

The calculated adsorption energies (ΔE_{ads}) for NH_3, $MeNH_2$, Me_2NH and Me_3N in H-[Ga]MOR are given in Table 4, and the proton affinities, compared with their experimental values as well as the corresponding pK_a of their conjugate acid are also presented. It is worth noting that since there is small difference between the acid strength of H-[Ga]MOR and H-[Al]MOR, we use the experimental values of the amines adsorption energies in H-[Al]MOR as standard to validate our results.

From the proton affinity (PA) of free amines in Table 4, it can be seen that in the gas phase, the relative basicity of these amine molecules follows the order: $NH_3 < MeNH_2 < Me_2NH < Me_3N$, due to the inductive effect of alkyl groups. While on the basis of the pK_a of their conjugate acids [33], the basicity increases in the order: $NH_3 < Me_3N < MeNH_2 < Me_2NH$, which resulted from the solvent effects. Here, when measured by their adsorption energies on acidic zeolites, the basicity of these amines increases in the order of $NH_3 < MeNH_2 < Me_3N < Me_2NH$, which is in agreement with the order of their experimental adsorption energies in acidic zeolites [34], but is different from the basicity order in both the gas phase and solvents. All three measurements identify NH_3 as the least basic probe, but the orders of the substituted amines differ from each other. This difference reflects the role of counterion on one hand, and on the other hand, the interaction between $[R_3NH]^+$ and the counterion, which is the negatively charged framework in zeolite. The interplay between $[R_3NH]^+$ and the negatively charged zeolite framework includes not only the electrostatic and hydrogen bonds interaction but also steric interaction.

The order of the adsorption energies of amines in H-[Ga]MOR calculated in this work is the same as that in H-

Table 4
The adsorption energies of amines (kcal/mol) in the H-[Ga]MOR clusters (ZeOH) of A and B, proton affinities (kcal/mol) of the free amines, compared with their experimental values and the corresponding pK_a of the conjugate acid of amines

	NH_3/ZeOH	$MeNH_2$/ZeOH	Me_2NH/ZeOH	Me_3N/ZeOH
ΔE_{relat}[a]	−2.3	0.0	7.3	4.1
ΔE_{ads} (calc. A)	42.2	44.6	56.2	50.2
ΔE_{ads} (calc. B)	40.9	41.0	45.3	42.6
ΔE_{ads} (Expt. [34])[b]	38.2	47.8	53.8	52.6
ΔE_{ads} (calc. [35])[b]	32.4	37.6	45.7	44.5
PA (Expt. [37])	204.0	214.1	220.6	225.1
PA (calc. [38])	202.4	213.3	220.5	224.9
pK_a [33]	9.3	10.6	10.7	9.7

[a] The relative total energies of the adsorption complexes in B as compared for A.
[b] The experimental and calculated ΔE_{ads} of amines in H-[Al]MOR, respectively.

Table 5
B3LYP/6-31G(d) stretching frequencies of N—H and C—H bonds of amines in the gas phase and adsorbed states in A[a]

	NH_3(g)[b]	NH_4^+(g)[b]	NH_4^+(ads)	$\Delta\upsilon$[c]
N—H	3431, 3430, 3303	3351, 3349, 3348, 3233	3438, 3119, 3055, 2865	87, −230, −293, −368
	$MeNH_2$(g)	$MeNH_3^+$(g)	$MeNH_3^+$(ads)	$\Delta\upsilon$
N—H	3411, 3331	3344, 3343, 3261	3379, 2875, 2739	35, −468, −522
C—H	2998, 2960, 2855	3096, 3096, 3095	3095, 3062, 2981	−1, −34, −15
	Me_2NH(g)	$Me_2NH_2^+$(g)	$Me_2NH_2^+$(ads)	$\Delta\upsilon$
N—H	3359	3334, 3283	3336, 2874	2, −409
C—H	2997, 2996, 2951, 2950, 2833, 2826	3087, 3086, 3083, 3083, 2988, 2986	3214, 3191, 3176, 3171, 3089, 3083	3, −19, −30, −35, −19, −23
	Me_3N(g)	Me_3NH^+(g)	Me_3NH^+(ads)	$\Delta\upsilon$
N—H	–	3298	2682	−616
C—H	2999, 2999, 2994, 2958, 2953, 2953, 2824, 2807, 2806	3079, 3079, 3079, 3077, 3076, 3075, 2985, 2981, 2980	3109, 3081, 3077, 3072, 3057, 3054, 2980, 2969, 2965	30, 2, −2, −4, −19, 2, −5, −12, −15

[a] All the frequencies presented here have been scaled by 0.9613.
[b] Ref. [35].
[c] $\Delta\upsilon$ is the frequency shift between amines adsorbed in H-[Ga]MOR and free protonated amines.

[Al]MOR of our earlier calculation data [35]. It is interesting to note that the calculation results in this work also agree well with the experimentally determined adsorption energies for H-[Al]MOR [34]. The averaged difference for the most stable complexes is 2.7 kcal/mol on one hand, and on the other hand, this nice agreement provides the opportunity to identify the most favored acidic site to adsorb amines. For NH_3, NH_4^+/A has larger ΔE_{ads}, but is less close to the experimental value than NH_4^+/B, and the latter structure is more stable than the former. Therefore B is the most favored site for NH_3 adsorption. For Me_2NH and Me_3N, both $Me_2NH_2^+$/A and Me_3NH^+/A have ΔE_{ads} more close to the experimental values and are more stable than $Me_2NH_2^+$/B and Me_3NH^+/B. Therefore, A is the most favored site for Me_2NH and Me_3N adsorption. However, for $MeNH_2$, both $MeNH_3^+$/A and $MeNH_3^+$/B have the same total energy, and the adsorption energies ΔE_{ads} from A and B is close to each other, thus $MeNH_2$ can be in equilibrium between A and B. These results show the correlation between structure/energy and acidity.

In addition, the calculated adsorption energies for amines/H-[Al]MOR < amines/H-[Ga]MOR, parallels the order of NH_4^+/[Al]ZSM-5 < NH_4^+/[Ga]ZSM-5 [36]. This energetic changes are reflected by the structural parameters of the adsorption complexes of NH_3 in H-[Ga]MOR and H-[Al]MOR. For example, most of the bond lengths of H-bond interactions are shorter in H-[Ga]MOR (A: 1.730, 1.875 and 2.126 Å) than that in H-[Al]MOR (2.408, 2.037 and 1.586 Å) [35], indicating the stronger interaction in the former than in the latter. As for the substituted amines, it is shown that the hydrogen bond interaction in the $[HNR_3^+]$/[Ga]MOR complexes are stronger than that in $[HNR_3^+]$/[Al]MOR complexes, as reflected by the O–H bond lengths as well as the numbers of the H-bonds formed (see Table 2, Ref. [35]). These results confirm the claim by Brändle and Sauer [15] and Gorte and coworkers [36] that the adsorption energies of amines depend not only on the energy of deprotonation of the zeolite (the acidity of the zeolites) but also on the proton affinities of amines and the interaction energy of the ammonium ion with the negatively charged framework.

3.5. IR frequencies

The adsorption energy is considered as one of the most valuable data obtained from experimental observation which can be used to validate the theoretical results [19]. Thus we used 6T clusters (Fig. 5) cut from the adsorption complexes based on A, which gives the adsorption energies much closer to the experimental data, to carry out frequency analysis calculations. These 6T clusters representing the adsorption complexes are cut from the high layer of ONIOM2 models in which all the interactions are included, and are optimized at B3LYP/6-31G(d,p) level. The calculation results are listed in Table 5. In order to analyze the interaction of amines with the zeolite framework, it is necessary to compare the IR frequencies of free R_3NH^+(g) with the adsorbed R_3NH^+(ads). It is to be noted that the IR frequencies of free R_3N(g) and free R_3NH^+(g) published previously [35] are also given here only for comparison.

The strength of the interaction between R_3NH^+ and the zeolite framework can be estimated by comparing the N–H and C–H IR frequencies of R_3NH^+(g) and R_3NH^+(ads), as given in Table 5. The largest shifts are found for the N–Hz bonds, which have strong hydrogen bonds interaction with the bridging oxygen atom (Oz), e.g., down shift of 368 cm^{-1} for NH_4^+(ads), 522 cm^{-1} for $MeNH_3^+$(ads), 409 cm^{-1} for $Me_2NH_2^+$(ads) and 616 cm^{-1} for Me_3NH^+(ads). These changes agree with the variation of the $R_{Oz—Hz}$ and $R_{N—Hz}$ distances (Table 2). The shifts of the other hydrogen bonding are relatively small. When compared with the R_3NH^+(g), most of the C–H frequencies in the adsorbed states are shifted

downward by small values, indicating that the interaction between the lattice oxygen atoms and C–H bonds are minor as compared with that of the N–H bonds.

4. Conclusions

The adsorption of four amines, NH_3, $MeNH_2$, Me_2NH, and Me_3N in H-[Ga]MOR are investigated by the two-layered ONIOM computational method. It is shown that there are two stable bridging oxygen sites in the framework for charge-compensating proton to form the Brønsted acid sites (O_2 and O_{10}). Upon the adsorption in these two acidic sites, the amine molecules are all protonated by the acidic proton of H-[Ga]MOR and form the ion-pair adsorption complexes. In addition to the hydrogen bonds between hydrogen atoms bonded to nitrogen and the negatively charged framework oxygen atoms, there also exist weaker interactions between the methyl hydrogen atoms and the framework oxygen atoms (apart from NH_4^+). In addition, the calculated adsorption energies of amines agree reasonably with the experimental data, and it is shown that NH_3 prefers to adsorb at the O_2H site, while Me_2NH and Me_3N prefer to adsorb at the $O_{10}H$ site, and $MeNH_2$ can be in equilibrium between O_2H and $O_{10}H$. This is due to the effect of introduced methyl groups and the different basicity and structures of these amines. Based on the order of the adsorption energies, the basicity of the adsorbed amines in zeolite differs from that in the gas phase (proton affinities) and in solution (pK_a values). The N–H stretching frequencies of the adsorbed R_3NH^+ are computed to be up-shifted, as compared to those of the free protonated forms.

Acknowledgments

The authors are grateful to National Natural Science Foundation of China (No. 20403028) and The State Key Fundamental Research Project as well as Chinese Academy of Sciences for the financial support, and to the Alexander von Humboldt Foundation for the donation of computing facilities.

References

[1] C. Bigey, B.-L. Su, J. Mol. Chem. A 209 (2004) 179.
[2] L.V. Pirutko, A.K. Uriarte, V.S. Chernyavsky, A.S. Kharitonov, G.I. Panov, Micropor. Mesopor. Mater. 48 (2001) 345.
[3] E.J.M. Hensen, Q. Zhu, R.A. van Santen, J. Catal. 220 (2003) 260.
[4] Z.K. Xie, Q.L. Chen, C.F. Zhang, J.Q. Bao, Y.H. Cao, J. Phys. Chem. B 104 (2000) 2853.
[5] R. Barthos, F. Lónyi, Gy. Onyestyák, J. Valyon, J. Phys. Chem. B 104 (2000) 7311.
[6] S. Lim, G.L. Haller, J. Phys. Chem. B 106 (2002) 8437.
[7] W. Daniell, N.-Y. Topsoe, H. Knozinger, Langmuir 17 (2001) 6233.
[8] F. Docquir, V. Norberg, H. Toufar, J.-L. Paillaud, B.L. Su, Langmuir 18 (2002) 5963.
[9] F. Docquir, H. Toufar, B.L. Su, Langmuir 17 (2001) 6282.
[10] J. Limtrakul, P. Khongpracha, S. Jungsuttiwong, T.N. Truong, J. Mol. Catal. A 153 (2000) 155.
[11] S.J. Cook, A.K. Chakraborty, A.T. Bell, D.N. Theodoru, J. Phys. Chem. 97 (1993) 6679.
[12] A.H. de Vries, P. Sherwood, S.J. Collins, A.M. Rigby, M. Rigutto, G.J. Kramer, J. Phys. Chem. B 103 (1999) 6133.
[13] R.C. Deka, K.J. Hirao, J. Mol. Catal. 181 (2002) 275.
[14] U. Eichler, M. Brändle, J. Sauer, J. Phys. Chem. B 101 (1997) 10035.
[15] M. Brändle, J. Sauer, J. Am. Chem. Soc. 120 (1998) 1556.
[16] F. Maseras, K. Morokuma, J. Comput. Chem. 16 (1995) 1170.
[17] S. Dapprich, I. Komáromi, K.S. Byun, K. Morokuma, M.J. Frisch, J. Mol. Struct. (TheoChem) 461/462 (1999) 1.
[18] G.S. Tschumper, K. Morokuma, J. Mol. Struct. (TheoChem) 592 (2002) 137.
[19] S. Kasuriya, A. Namuangruk, P. Treesukol, M. Tirtowidjojo, J. Limtrakul, J. Catal. 219 (2003) 320.
[20] I. Roggero, B. Civalleri, P. Ugliengo, Chem. Phys. Lett. 341 (2001) 625.
[21] X. Solans-Monfort, J. Bertran, V. Branchadell, M. Sodupe, J. Phys. Chem. B 106 (2002) 10220.
[22] A. Damin, F. Bonino, G. Ricchiardi, S. Bordiga, A. Zecchina, C. Lamberti, J. Phys. Chem. B 106 (2002) 7524.
[23] J.A. van Bokhoven, M. Tromp, D.C. Koningsberger, J.T. Miller, J.A.Z. Pieterse, J.A. Lercher, B.A. Williams, H.H. Kung, J. Catal. 202 (2001) 129.
[24] M.D. Macedonia, D.D. Moore, E.J. Maginn, M.M. Olken, Langmuir 16 (2000) 3823.
[25] K. Yamagishi, S. Namba, T. Yashima, J. Phys. Chem. 95 (1991) 872.
[26] M. Dong, J. Wang, Y. Sun, Micropor. Mesopor. Mater. 43 (2001) 237.
[27] S.P. Yuan, J.G. Wang, Y.W. Li, S.Y. Peng, J. Mol. Catal. A 175 (2001) 131.
[28] M.M.J. Treacy, J.B. Higgins, R. von Ballmoos, Zeolites 16 (1996) 751.
[29] Gaussian 03, Revision B.04, Gaussian Inc., Pittsburgh, PA, 2003.
[30] J.B. Foresman, Æ. Frisch, Exploring Chemistry with Electronic Structure Methods, 2nd ed., Gaussian Inc., Pittsburgh, PA, 64 pp.
[31] M. Sierka, J. Sauer, J. Phys. Chem. B 105 (2001) 1603.
[32] S.P. Yuan, J.G. Wang, Y.W. Li, H.J. Jiao, J. Mol. Struct. 674 (2004) 267.
[33] F.A. Carey, Organic Chemistry, McGraw-Hill, New York, 2003, p. 920.
[34] C. Lee, D.J. Parrillo, R.J. Gorte, W.E. Farneth, J. Am. Chem. Soc. 118 (1996) 3262.
[35] N. Jiang, S.P. Yuan, J.G. Wang, H. Jiao, Z.F. Qin, Y.-W. Li, J. Mol. Catal. A 220 (2004) 221.
[36] D.J. Parrillo, C. Lee, R.J. Gorte, J. Phys. Chem. 99 (1995) 8745.
[37] R.S. Drago, T.R. Cundari, D.C. Ferris, J. Org. Chem. 54 (1989) 1042.
[38] H. Jiao, J.-F. Halet, J.A. Gladysz, J. Org. Chem. 66 (2001) 3902.